Predictive Value of ^{18}F-FDG PET in Patients with Advanced Medullary Thyroid Carcinoma Treated with Vandetanib

Rudolf A. Werner[1,2], Jan-Stefan Schmid[1], Takahiro Higuchi[1,3], Mehrbod S. Javadi[2], Steven P. Rowe[2], Bruno Märkl[4], Christoph Aulmann[5], Martin Fassnacht[6,7], Matthias Kroiss[6,7], Christoph Reiners[1], Andreas K. Buck[1], Michael C. Kreissl*[8,9], and Constantin Lapa*[1]

[1]Department of Nuclear Medicine, University Hospital, University of Würzburg, Würzburg, Germany; [2]Division of Nuclear Medicine and Molecular Imaging, Russell H. Morgan Department of Radiology and Radiological Science, Johns Hopkins University School of Medicine, Baltimore, Maryland; [3]Department of Bio-Medical Imaging, National Cardiovascular and Cerebral Research Center, Osaka, Japan; [4]Institute for Pathology, Hospital Augsburg, Augsburg, Germany; [5]Medical Department II, Hospital Augsburg, Augsburg, Germany; [6]Comprehensive Cancer Center Mainfranken, University of Würzburg, Würzburg, Germany; [7]Division of Endocrinology and Diabetes, Department of Internal Medicine I, University Hospital, University of Würzburg, Würzburg, Germany; [8]Department of Nuclear Medicine, Hospital Augsburg, Augsburg, Germany; and [9]Department of Radiology and Nuclear Medicine, University Hospital Magdeburg, Magdeburg, Germany

Medullary thyroid carcinoma (MTC), which originates from parafollicular, calcitonin-secreting cells, accounts for approximately 5% of all thyroid cancers (*1*). Because MTC cells do not accumulate radioiodine (*1*), surgery represents the only curative strategy in early disease stages. In advanced disease stages, the only treatment option formerly available was cytotoxic chemotherapy, which is associated with low response rates (*2,3*). In the last decade, however, tyrosine kinase inhibitors (TKIs) have led to a paradigm shift: vandetanib and cabozantinib were approved for the treatment of advanced MTC after successful phase 3 trials (*4–6*). In one of these trials, for example, vandetanib demonstrated favorable antitumor activity, with disease control rates in 73% of patients and confirmed objective partial responses in 20% (*4*). However, there was no prolongation of overall survival (OS) (*4*), and adverse effects, including diarrhea, cutaneous reactions, hypertension, and even life-threatening cardiac arrhythmias, have been described and demand close patient monitoring (*7*). Given the more widespread use of TKI, reliable predictors of TKI responders before treatment initiation are intensely sought after (*8*).

The prognostic value of baseline ^{18}F-FDG PET/CT assessment before TKI initiation has been shown in several types of cancers, such as renal cell carcinoma and gastrointestinal stromal tumor (*9,10*). Additionally, in iodine-refractory differentiated thyroid cancer scheduled for sunitinib treatment, early reduction of metabolic activity was associated with a morphologic response (*11,12*).

In this bicentric study, we aimed to elucidate the prognostic role of ^{18}F-FDG PET/CT in MTC patients at the start of vandetanib treatment.

MATERIALS AND METHODS

Patient Population

All patients underwent imaging for clinical purposes and gave written informed consent to the diagnostic and therapeutic procedures.

For correspondence or reprints contact: Constantin Lapa, Department of Nuclear Medicine, University Hospital Würzburg, Oberdürrbacherstrasse 6, 97080 Würzburg, Germany.
E-mail: lapa_c@ukw.de
*Contributed equally to this work.

The requirement for additional approval was waived by the local institutional review boards because of the retrospective character of this study. All patients also gave written informed consent for the recording and anonymized analysis of their data. Parts of this cohort received vandetanib in a clinical trial (*5*).

Between April 2007 and July 2016, 18 patients (12 men and 6 women; median age, 48 y; range, 28–78 y) with advanced, progressive MTC were started on vandetanib (300 mg orally per day) at the University Hospital of Würzburg ($n = 14$) or the Hospital of Augsburg ($n = 4$), Germany. All patients had undergone previous therapies, including surgery (all patients), external-beam radiation therapy (4/18, 22.2%), chemotherapy (3/18, 16.7%), transarterial chemoembolization (2/18, 11.1%), radioiodine therapy (1/18, 5.6%; patient 16, initially misclassified as having differentiated thyroid cancer), or sorafenib (1/18, 5.6%). Detailed patient information is given in Table 1.

Imaging-Based Response Assessment

Treatment response was assessed every 3 mo according to RECIST, version 1.1, based on CT findings (*13*), and the RECIST measurements were confirmed by an attending radiologist (*14*). During follow-up, the best response achieved by CT criteria (complete response, partial response, stable disease, or progressive disease) was evaluated. Progression-free survival (PFS) was defined according to RECIST by serial radiologic assessment starting from the time of TKI initiation (*13*). For OS, the interval between the start of treatment and the date of death was used. Data were censored on August 1, 2016.

Imaging

In 4 (22.2%) of 18 patients, dedicated PET was performed on a stand-alone lutetium oxyorthosilicate full-ring PET scanner (ECAT Exact 47; Siemens Medical Solutions). In the remaining patients, integrated PET/CT was performed. Twelve (85.7%) of 14 patients were scanned on a Biograph mCT PET/CT system (Siemens Medical Solutions), and 2 (14.3%) of 14 were scanned on a Gemini TF 16 PET/CT system (Philips). Before image acquisition, the patients fasted for at least 6 h, and their blood glucose levels were less than 160 mg/dL. ^{18}F-FDG was injected intravenously. After 60 min, transmission data were acquired from the base of the skull to the proximal thighs using ^{68}Ge rod sources (in the case of the stand-alone PET scanner) or spiral CT, either with intravenous contrast enhancement (13 patients [92.9%], dose modulation with a quality reference of 210 mAs, 120 kV, 512 × 512 matrix, and 5-mm slice thickness) or without intravenous contrast enhancement (1 patient [7.1%], 80 mAs, 120 kV, 512 × 512 matrix, and 5-mm slice thickness). Consecutively, the PET emission data were acquired. After decay and scatter correction, the PET data were reconstructed iteratively with attenuation correction, using the algorithm supplied by the scanner manufacturer.

After 3 mo, ^{18}F-FDG PET/CT was performed on 16 (88.9%) of 18 patients, and CT was performed on 1 (5.6%) of 18 patients. In the remaining patient, imaging-based follow-up was not available because of early therapy termination due to adverse events.

Imaging Interpretation

For both the baseline and the follow-up scans, the axial PET image slice displaying the maximum uptake was selected, and a 3-dimensional volume of interest was drawn around the whole tumor area. A standardized 15-mm circular region of interest was then placed over the area with the peak activity. This region of interest was used to derive the respective SUV_{mean} and SUV_{max}. The radiotracer concentration in the region of interest was decay-corrected and normalized to the injected dose per kilogram of patient body weight.

TABLE 1
Detailed Patient Characteristics

Patient no.	Sex	Age (y)	Metastatic sites	Disease type	Prior therapy	Somatic RET mutation
1	F	57	LN, lung, liver	Sporadic	Surgery	Unknown
2	F	59	LN, liver	Sporadic	Surgery, CTx, TACE	Negative
3	M	41	LN, bone	Sporadic	Surgery, CTx	Unknown
4	M	50	LN, lung	Sporadic	Surgery	Unknown
5	F	20	LN, lung, liver	Sporadic	Surgery	Negative
6	M	57	LN, lung, liver, bone	Hereditary	Surgery, TACE	—
7	M	40	LN, lung	Sporadic	Surgery, CTx	Unknown
8	M	40	LN, liver, bone	Sporadic	Surgery	Negative
9	F	35	LN, lung	Sporadic	Surgery	Negative
10	M	59	LN, lung	Sporadic	Surgery	Unknown
11	M	30	LN	Sporadic	Surgery, RTx	Negative
12	M	47	LN, liver, bone, soft tissue, pancreatic infiltration	Sporadic	Surgery	Unknown
13	M	54	LN, lung, liver	Sporadic	Surgery	Unknown
14	M	78	LN, lung, bone	Sporadic	Surgery	Unknown
15	F	49	LN, liver, bone	Sporadic	Surgery, RTx	Positive
16	F	28	LN, bone	Sporadic	Surgery, radioiodine therapy*, RTx	Positive
17	M	46	Liver, bone	Sporadic	Surgery, sorafenib	Unknown
18	M	55	LN, lung, bone, soft tissue	Sporadic	Surgery, RTx	Positive

*Initially classified as differentiated thyroid carcinoma.
LN = lymph node; CTx = chemotherapy; TACE = transarterial chemoembolization; RTx = radiation therapy.

Tumor Markers

Serum levels of carcinoembryonic antigen (CEA, mg/L) and calcitonin (pg/mL) were measured before baseline using dedicated radioimmunoassays (*14*). Between 3 and 22 determinations (median, 6 determinations) were available per patient. Tumor marker doubling times were calculated using the American Thyroid Association calculator (*3*).

Clinical Parameters

The following clinical parameters were obtained: sex, age, metastatic sites at time of baseline PET, prior therapy, and tumoral rearranged-during-transfection (RET) mutation status (Table 1).

Analysis and Statistics

Statistical analyses were performed using PASW Statistics software (version 22.0; SPSS, Inc.). Quantitative values were expressed as mean ± SD and range as appropriate. The 2-tailed paired Student *t* test was used to compare differences between dependent groups, and the 2-tailed independent Student *t* test was used to compare differences between independent groups. Cox multiparametric regression analysis was applied to determine independent prognostic parameters. Cutoffs for the prediction of imaging-based PFS and OS were determined by receiver-operating-characteristic (ROC) analysis using the Youden Index for maximization of specificity and sensitivity (*15,16*). Pearson correlation was used to determine the association of tumor marker levels with other PET parameters and with PFS and OS. Kaplan–Meier analysis was performed using thresholds established by ROC analysis when the ROC analysis showed statistically significant results. Nonparametric log-rank tests were used to assess differences in the Kaplan–Meier curves. A P value of 0.05 or less was considered statistically significant. To adjust for multiple testing, Bonferroni adjustment was performed.

RESULTS

Baseline ^{18}F-FDG PET results were positive in all patients. Of the 18 patients, 17 (94.4%) presented with lymph node metastases; 10 (55.6%), with lung metastases; 9 (50.0%), with liver lesions; 9 (50.0%), with bone lesions; 2 (11.1%), with soft-tissue metastases; and 1 (5.6%), with tumor infiltration of the pancreas.

One patient had hereditary medullary thyroid cancer (patient 6, with multiple endocrine neoplasia 2A syndrome). In the nonhereditary cases, somatic RET mutations were detected in 3 (37.5%) of 8 patients, in whom somatic RET mutational status was determined (Table 1).

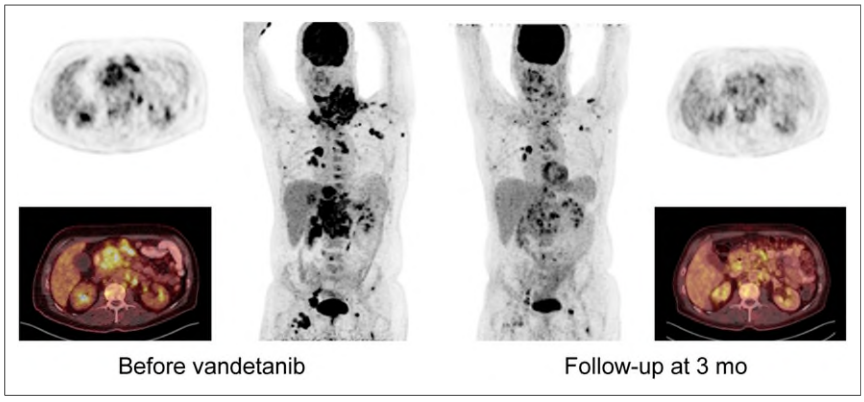

FIGURE 1. A 47-y-old man (patient 12) with extensive tumor load. Before TKI initiation, patient presented with highly aggressive disease on ^{18}F-FDG PET, with SUV_{mean} of 13.4 for hottest lesion (right clavicular lymph node). After 3 mo of vandetanib, partial response could be detected, with 54.5% decline in metabolic activity (SUV_{mean}, 6.1). However, because of disease aggressiveness, patient died 11 mo after start of treatment.

The best morphologic response according to RECIST was classified as follows: stable disease in 8 (44.4%) of 18, partial response in 8 (44.4%) of 18, and complete response in 1 (5.6%) of 18. In the remaining patient, response could not be assessed because of early therapy termination. During follow-up (median, 5.2 y; range, 1.8–9.3 y), 9 patients (50%) experienced disease progression after a median of 2.1 y (range, 3 mo–9.1 y), whereas the remainder exhibited ongoing disease control. Eight of the progressive-disease patients died from their disease (median, 3.5 y; range, 11 mo–9.1 y) during follow-up.

Correlation of Serum Tumor Marker Doubling Times and Clinical Parameters with PFS and OS

The doubling times were highly variable among patients and ranged from 1.7 mo to 2.4 y for calcitonin and 1.4 mo to 5.1 y for CEA. The median calcitonin and CEA doubling times were 6.8 and 8.3 mo, respectively. Longer CEA doubling times were significantly related to a longer PFS and OS ($r = 0.7$ and 0.76, respectively; $P < 0.01$), whereas no correlation was observed for calcitonin.

The investigated clinical parameters (sex, age, metastatic sites at time of baseline PET, prior therapy, and RET mutation status) as given in Table 1 did not significantly correlate with PFS or OS.

Imaging-Based Findings of ^{18}F-FDG Baseline and Follow-up PET

At baseline, 10 lymph node and 6 visceral metastases were identified as the metabolically most active lesions. Median $SUV_{mean/max}$ was 4.6 (range, 3.2–27.4) and 7.4 (range, 3.8–37.5), respectively.

As derived by ROC analysis, an SUV_{mean} of more than 4.0 at baseline was correlated with a PFS significantly shorter (1.9 y) than that (5.2 y) for patients with lower metabolic activity ($P = 0.04$; area under the curve, 0.76), whereas no significant correlation was observed for SUV_{max} ($P = 0.06$). Both parameters failed to predict OS (SUV_{mean}, $P = 0.2$; SUV_{max}, $P = 0.3$).

At follow-up, the above-mentioned lymph node and visceral metastases were reanalyzed. SUV_{mean} dropped to a median of 3.0 (range, 2.1–6.6), with a median reduction of 26.9%. For SUV_{max}, a 25.6% reduction to a median of 3.8 (range, 2.2–16.3) was observed (Fig. 1; Table 2; Supplemental Table 1 [supplemental materials are available at http://jnm.snmjournals.org]).

Whereas sustained high ^{18}F-FDG uptake with an SUV_{mean} of more than 2.8 tended to correlate with a shorter PFS of 1.9 y (vs. 3.5 y for $SUV_{mean} < 2.8$; $P = 0.3$), the differences did not reach statistical significance. In parallel to baseline, no significant correlation was observed for SUV_{max} ($P = 0.2$), and both SUV_{mean} and SUV_{max} failed to predict OS ($P = 0.3$, $P = 0.2$, respectively).

In addition, the extent of metabolic activity reduction between baseline and 3-mo follow-up PET was not predictive for either PFS ($P = 0.2$) or OS ($P = 0.4$).

The results of ROC analysis, including the area under the curve, sensitivity, specificity, and dedicated thresholds for each group (>cutoff vs. <cutoff), can be found in Table 3.

Kaplan–Meier Analysis

Kaplan–Meier analysis revealed a significant distinction between high- and low-risk

TABLE 2
$SUV_{mean/max}$ of Baseline and Follow-up ^{18}F-FDG PET Scans and Changes Between Them

Parameter	SUV_{mean}	SUV_{max}
Baseline PET*	4.6 (3.2–7.4)	7.4 (3.8–37.5)
Follow-up PET†	3 (2.1–6.6)	3.8 (2.2–16.3)
Change between baseline and follow-up in 12/16 patients (%)	26.9 (7.7–70)	25.6 (15.4–69.2)

*Location of investigated visceral metastases: 5 cervical, 2 mediastinal, 2 hilar, and 1 clavicular lymph node; 3 bone; 2 liver; and 1 lung.
†Location of investigated visceral metastases: 5 cervical, 2 mediastinal, 2 paratracheal, and 1 hilar lymph node; 4 bone; 1 liver; and 1 lung.
Data are median followed by range in parentheses.

patients for PFS using a threshold of 4 for SUV_{mean} on baseline PET as derived by ROC analysis ($P < 0.05$); the respective Kaplan–Meier-plots are given in Figure 2.

DISCUSSION

In this the largest, but still relatively small, patient cohort published to date, we report on the prognostic value of ^{18}F-FDG in patients with advanced MTC at the start of TKI treatment. Interestingly, even though MTC is known to have a variable (and often even negative) ^{18}F-FDG uptake in tumor lesions (*17,18*), all patients of our cohort had at least 1 hypermetabolic metastatic lesion.

A high ^{18}F-FDG uptake at baseline had prognostic implications in terms of a significantly shorter PFS. An SUV_{mean} of more than 4.0 for the metabolically most active lesion was associated with an almost 2.7-fold shorter PFS (1.9 vs. 5.2 y). The percentage of tumor metabolism reduction after 3 mo of TKI treatment did not offer prognostic value, and ^{18}F-FDG failed to predict OS. This finding may be explained by the limited number of patients enrolled in this study. Additionally, vandetanib leads to reduced tumor proliferation, angiogenesis, and metastasis by inhibition of various tyrosine kinases but does not necessarily induce cell death (*19,20*).

In line with this consideration, Walter et al. have demonstrated the early transcriptional downregulation of key genes in glycolysis pathways such as STAT3 and Grb7/10 as soon as 3 d after vandetanib treatment initiation (*20*). However, this decline did not seem to be related to cell death, as no increase in apoptotic cells was detected in vitro (*20*). Since the main aim of vandetanib treatment is disease stabilization rather than cure, ^{18}F-FDG PET/CT could be used as a noninvasive tool to identify high-risk patients with more aggressive disease who need to be monitored more closely than those with low ^{18}F-FDG uptake at baseline.

Interestingly, clinical parameters such as age, sex, sites of metastases, prior therapy, and RET mutation status failed to predict response. The usefulness of analysis of serum marker doubling times as indicators of disease aggressiveness has been shown by several studies (*21,22*); however, in our study, only pretherapeutic CEA doubling times were strongly correlated with both PFS and OS, whereas no relation to calcitonin was observed, perhaps also because of the small sample size.

Like ^{18}F-FDG in our cohort, serum marker follow-up of thyroid cancer patients undergoing TKI treatment has been reported to be complicated by the phenomenon of tumor marker fluctuations not necessarily denoting true tumor escape. In contrast, morphologically measurable disease progression could be confirmed only after a series of subsequent rises in serum markers (*14,23,24*). Given the earlier time point of response prediction obtainable, ^{18}F-FDG PET might serve treating physicians outside the scenario of controlled studies as a suitable tool for therapy monitoring and patient-tailored decisions.

TABLE 3
Results of ROC Analysis for SUV_{mean} and SUV_{max} as Obtained by ^{18}F-FDG PET

Parameter	*P*	Cutoff	Sensitivity (%)	Specificity (%)	AUC	Above cutoff	Below cutoff
SUV_{mean}, PFS							
Baseline	0.04*	4.0	88.9	62.5	0.76	1.9 y (12/18)	5.2 y (6/18)
Follow-up	0.28	2.8	71.4	62.5	0.6	1.9 y (9/16)†	3.5 y (7/16)†
SUV_{mean}, OS							
Baseline	0.2	6.9	37.5	100	0.63	2.0 y (3/18)	3.8 y (15/18)
Follow-up	0.28	2.8	62.5	71.4	0.6	2.8 y (9/16)†	3.6 y (7/16)†
SUV_{max}, PFS							
Baseline	0.06	7.25	77.8	75	0.74	2.0 y (9/18)	3.5 y (9/18)
Follow-up	0.19	2.7	85.7	50	0.64	1.8 y (11/16)†	3.5 y (5/16)†
SUV_{max}, OS							
Baseline	0.28	16.85	25	100	0.59	1.5 y (2/18)	3.7 y (16/18)
Follow-up	0.21	2.7	85.7	44.4	0.63	3.6 y (11/16)†	3.6 y (5/16)†

*Significant according to ROC analysis.
†2 patients lost to PET-based follow-up.
Data in parentheses are numbers of patients.

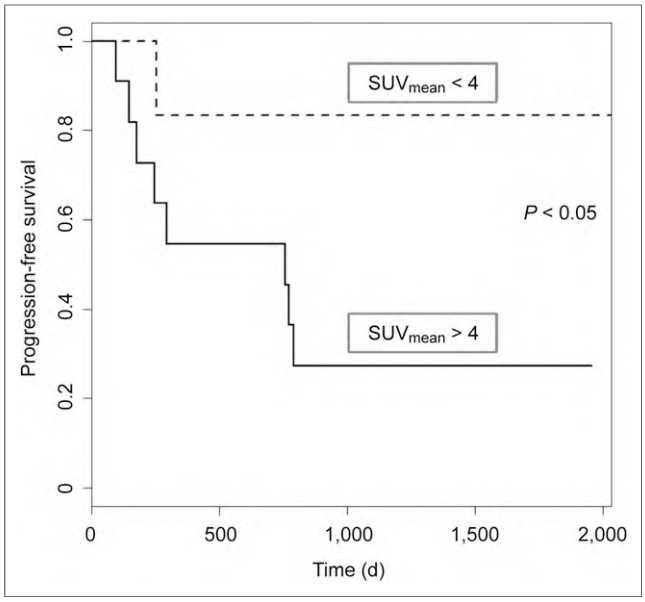

FIGURE 2. Kaplan–Meier plots for probability of PFS using SUV_{mean} of baseline ^{18}F-FDG PET. High-risk group is indicated by solid line. Cutoff of 4 derived by ROC analysis was used (Table 3).

Additionally, in comparison with the cohort of an earlier phase 3 vandetanib trial by Wells et al. (*5*), our study population had more advanced and progressive disease, since our PFS was shorter than that in the prior study (30.5 mo). Moreover, fairly short median calcitonin and CEA doubling times of 6.8 and 8.3 mo, respectively, before initiation of treatment were found in our patient cohort. Hence, because more aggressive tumors were treated in our study than in the phase 3 trial (*5*), we could achieve a response rate of up to 50% (8 partial responses and 1 complete response). This rate indicates that vandetanib leads to tumor control and that the included patients most likely benefited from the treatment; however, this possibility cannot be verified in the absence of a control arm. In addition, even in a patient with a slightly increased SUV_{mean} at baseline (patient 18, Supplemental Table 1), vandetanib initiation led to a complete disappearance of tumor burden. However, because of the underlying tumor biology, such an achieved response may persist only briefly.

This study had several limitations. Limiting its statistical power is the fact that only a small number of patients could be enrolled. Because the study was retrospective and bicentric, different PET scanners were used and the imaging protocols differed slightly between imaging centers. No additional partial-volume correction to reduce noise, including normalizing values to body surface area or to plasma glucose level, was performed. A future larger, multicentric prospective study is warranted to strengthen our preliminary results.

Additionally, in most the cases we did not determine the RET mutation status, which may represent another suitable predictor of PFS.

Last, potential intraindividual intertumoral heterogeneity regarding ^{18}F-FDG–negative, ^{68}Ga-DOTATATE–positive disease and its response to TKI treatment could not be assessed in this study but might be an interesting approach for further research (*25*).

CONCLUSION

^{18}F-FDG PET/CT can serve as a prognostic tool in patients with advanced MTC scheduled to undergo vandetanib treatment. An elevated glucose consumption as assessed by baseline PET was related to a shorter PFS; therefore, these patients need to be monitored more closely than those with a low ^{18}F-FDG uptake at baseline. Changes in ^{18}F-FDG uptake after 3 mo in this small group of patients failed to predict PFS and OS.

DISCLOSURE

This project received funding from the European Union's Framework Programme for Research and Innovation Horizon 2020 (2014–2020, no. 701983) under the Marie Skłodowska-Curie Grant Agreement. This project also received funding from the German Research Foundation (DFG) and the University of Wuerzburg in the funding program Open Access Publishing. Parts of this cohort received vandetanib while participating in the ZACTIMA trial. No other potential conflict of interest relevant to this article was reported.

ACKNOWLEDGMENTS

We thank all members of the laboratory and the PET teams of the nuclear medicine departments at Würzburg and Augsburg for their assistance. Additionally, we express our gratitude to Dr. Dirk O. Mügge (independent statistician, Göttingen, Germany) for his support in statistical analysis and to Johanna Vogt (Department of Nuclear Medicine, University Hospital Würzburg) for her assistance in data collection.

REFERENCES

1. Davies L, Welch HG. Increasing incidence of thyroid cancer in the United States, 1973-2002. *JAMA.* 2006;295:2164–2167.
2. Fassnacht M, Kreissl MC, Weismann D, Allolio B. New targets and therapeutic approaches for endocrine malignancies. *Pharmacol Ther.* 2009;123: 117–141.
3. Wells SA Jr, Asa SL, Dralle H, et al. Revised American Thyroid Association guidelines for the management of medullary thyroid carcinoma. *Thyroid.* 2015; 25:567–610.
4. Wells SA Jr, Gosnell JE, Gagel RF, et al. Vandetanib for the treatment of patients with locally advanced or metastatic hereditary medullary thyroid cancer. *J Clin Oncol.* 2010;28:767–772.
5. Wells SA Jr, Robinson BG, Gagel RF, et al. Vandetanib in patients with locally advanced or metastatic medullary thyroid cancer: a randomized, double-blind phase III trial. *J Clin Oncol.* 2012;30:134–141.
6. Elisei R, Schlumberger MJ, Muller SP, et al. Cabozantinib in progressive medullary thyroid cancer. *J Clin Oncol.* 2013;31:3639–3646.
7. Grande E, Kreissl MC, Filetti S, et al. Vandetanib in advanced medullary thyroid cancer: review of adverse event management strategies. *Adv Ther.* 2013;30:945–966.
8. Lenihan DJ, Kowey PR. Overview and management of cardiac adverse events associated with tyrosine kinase inhibitors. *Oncologist.* 2013;18:900–908.
9. Prior JO, Montemurro M, Orcurto MV, et al. Early prediction of response to sunitinib after imatinib failure by ^{18}F-fluorodeoxyglucose positron emission tomography in patients with gastrointestinal stromal tumor. *J Clin Oncol.* 2009; 27:439–445.
10. Vercellino L, Bousquet G, Baillet G, et al. ^{18}F-FDG PET/CT imaging for an early assessment of response to sunitinib in metastatic renal carcinoma: preliminary study. *Cancer Biother Radiopharm.* 2009;24:137–144.
11. Carr LL, Mankoff DA, Goulart BH, et al. Phase II study of daily sunitinib in FDG-PET-positive, iodine-refractory differentiated thyroid cancer and metastatic medullary carcinoma of the thyroid with functional imaging correlation. *Clin Cancer Res.* 2010;16:5260–5268.
12. Marotta V, Ramundo V, Camera L, et al. Sorafenib in advanced iodine-refractory differentiated thyroid cancer: efficacy, safety and exploratory analysis of role of serum thyroglobulin and FDG-PET. *Clin Endocrinol (Oxf).* 2013;78:760–767.

13. Eisenhauer EA, Therasse P, Bogaerts J, et al. New response evaluation criteria in solid tumours: revised RECIST guideline (version 1.1). *Eur J Cancer.* 2009; 45:228–247.
14. Werner RA, Schmid JS, Muegge DO, et al. Prognostic value of serum tumor markers in medullary thyroid cancer patients undergoing vandetanib treatment. *Medicine (Baltimore).* 2015;94:e2016.
15. Zou KH, O'Malley AJ, Mauri L. Receiver-operating characteristic analysis for evaluating diagnostic tests and predictive models. *Circulation.* 2007;115:654–657.
16. Youden WJ. Index for rating diagnostic tests. *Cancer.* 1950;3:32–35.
17. Skoura E, Datseris IE, Rondogianni P, et al. Correlation between calcitonin levels and [^{18}F]FDG-PET/CT in the detection of recurrence in patients with sporadic and hereditary medullary thyroid cancer. *ISRN Endocrinol.* 2012;2012: 375231.
18. Ong SC, Schoder H, Patel SG, et al. Diagnostic accuracy of ^{18}F-FDG PET in restaging patients with medullary thyroid carcinoma and elevated calcitonin levels. *J Nucl Med.* 2007;48:501–507.
19. Schlumberger M, Massicotte MH, Nascimento CL, Chougnet C, Baudin E, Leboulleux S. Kinase inhibitors for advanced medullary thyroid carcinoma. *Clinics (São Paulo).* 2012;67(suppl 1):125–129.
20. Walter MA, Benz MR, Hildebrandt IJ, et al. Metabolic imaging allows early prediction of response to vandetanib. *J Nucl Med.* 2011;52:231–240.
21. Laure Giraudet A, Al Ghulzan A, Auperin A, et al. Progression of medullary thyroid carcinoma: assessment with calcitonin and carcinoembryonic antigen doubling times. *Eur J Endocrinol.* 2008;158:239–246.
22. Barbet J, Campion L, Kraeber-Bodere F, Chatal JF, Group GTES. Prognostic impact of serum calcitonin and carcinoembryonic antigen doubling-times in patients with medullary thyroid carcinoma. *J Clin Endocrinol Metab.* 2005;90: 6077–6084.
23. Kurzrock R, Atkins J, Wheler J, et al. Tumor marker and measurement fluctuations may not reflect treatment efficacy in patients with medullary thyroid carcinoma on long-term RET inhibitor therapy. *Ann Oncol.* 2013;24:2256–2261.
24. Werner RA, Luckerath K, Schmid JS, et al. Thyroglobulin fluctuations in patients with iodine-refractory differentiated thyroid carcinoma on lenvatinib treatment: initial experience. *Sci Rep.* 2016;6:28081.
25. Conry BG, Papathanasiou ND, Prakash V, et al. Comparison of ^{68}Ga-DOTATATE and ^{18}F-fluorodeoxyglucose PET/CT in the detection of recurrent medullary thyroid carcinoma. *Eur J Nucl Med Mol Imaging.* 2010;37: 49–57.